

BEAM-BASED MEASUREMENT OF BROADBAND LONGITUDINAL IMPEDANCE AT NSLS-II *

V. Smaluk[†], A. Blednykh, G. Bassi, B. Bacha, Brookhaven National Laboratory, Upton, USA

Abstract

Interaction of a particle beam with the vacuum chamber impedance is one of the main effects limiting the beam intensity in accelerators. Minimization of the impedance is an essential part of the vacuum chamber design for any new accelerator project. The impedance can be estimated experimentally by measuring beam dynamics effects caused by the beam-impedance interaction. Experience obtained at many accelerator facilities shows the beam-based measurements are often different from the pre-computed impedance budgets, the discrepancy of a factor of two or even more is not unusual. The measurements of broadband longitudinal impedance carried out at NSLS-II are discussed in comparison with the numerically simulated impedance budget.

INTRODUCTION

For bunched particle beams, single-bunch collective effects of the beam dynamics are determined by integral parameters combining the broadband impedance of the vacuum chamber and the power spectrum of the beam. Such parameters are: the longitudinal / transverse effective impedance, the longitudinal loss factor, and the transverse kick factor. For analysis of the beam motion, both frequency-dependent impedance calculated by numerical simulations and simple approximate models, such as a broadband resonator or an inductive model, are used. The following effects depending on the beam intensity can be measured quite precisely with modern instruments and methods of beam diagnostics: bunch lengthening, synchronous phase shift, coherent shift of betatron frequencies, chromatic head-tail damping, orbit distortion by a local impedance.

For 15 storage rings, the beam-based measurements of the intensity-dependent bunch lengthening and betatron frequency shift, were analyzed [1]. The measured bunch lengthening was approximated by a modified Zotter equation (inductive model) [2], which is consistent with the Haissinski equation [3] (broadband resonator model). The betatron frequency shift was approximated by a linear formula, valid for small frequency shifts. The impedances derived from the beam measurements were compared with published impedance budgets. At best, the impedance budgets are consistent with the measurements with an accuracy of 20–30%, but in other cases the discrepancy may exceed 100%.

In the next chapters, we discuss beam-based measurements of the NSLS-II broadband longitudinal impedance and compare them with the impedance budget calculated using the electrodynamic simulation code GdfidL [4].

NSLS-II IMPEDANCE BUDGET

Now, the conventional way to calculate the impedance budget of a vacuum chamber is element-by-element computer simulation of wake fields excited by a model beam. The total frequency-dependent impedance of the whole ring chamber is a sum of the impedances of its components, assuming no interference of the wake fields excited by the beam in the adjacent components of the chamber.

Several 2D and 3D computer codes are now available to calculate the impedance of a vacuum chamber component with a complex shape. The codes simulate wake fields excited by a model beam with a predefined charge distribution (usually Gaussian) by solving Maxwell equations with boundary conditions determined by the geometry of the chamber. The code output is the wake potential V , which is a convolution of the wake function W (point-charge response) and the longitudinal charge density λ of the model bunch:

$$V(\tau) = \int_0^{\infty} W(t)\lambda(\tau - t)dt . \quad (1)$$

The impedance $Z(\omega)$ is calculated as

$$Z(\omega) = \frac{\tilde{V}(\omega)}{\tilde{\lambda}(\omega)} , \quad (2)$$

where \tilde{V} and $\tilde{\lambda}$ are the Fourier transforms of the wake potential and the longitudinal charge density, respectively.

As follows from equation (2), the bandwidth of the impedance obtained from the wake potential is limited by the spectrum width of the model bunch, which is inversely proportional to the bunch length. Thus, in order to calculate the impedance in a wide frequency band, the length of the model bunch must be very small. To obtain reliable results in the frequency bandwidth determined by the spectrum of a model bunch, the computational mesh size must also be small enough, substantially smaller than the bunch length.

For the NSLS-II storage ring, the impedance budget [5] was calculated using the GdfidL code [4]. All the vacuum chamber components with significant contribution to the total impedance were taken into account including synchrotron radiation absorbers, bellows, beam position monitors, transitions from the regular chamber to the RF cavity sections, dipole chambers, quadrupole and sextupole chambers, flanges, injection region, low-gap undulator chambers, beam scrapers, and resistive wall impedance. Total longitudinal impedance of NSLS-II is presented in Figure 1 together with the simplified models: broad-band resonator and pure inductive impedance. Spectra of the bunches with the length of 10 ps and 20 ps are also shown. For the broadband resonator, the shunt impedance $R_s = 9.45 \text{ k}\Omega$ and the

* Work supported by DOE under contract DE-SC0012704

[†] smaluk@bnl.gov

resonance frequency $\omega_r = 2\pi \times 28$ GHz are calculated by fitting the impedance calculated by GdfidL with the formula

$$Z_{\text{BBR}}(\omega) = \frac{R_s}{1 + iQ \left(\frac{\omega}{\omega_r} - \frac{\omega_r}{\omega} \right)}, \quad (3)$$

assuming the quality factor $Q = 1$. For the inductive model, the normalized impedance is

$$\frac{Z_{\parallel}}{n} = i \frac{R_s \omega_0}{Q \omega_r}, \quad (4)$$

where $n = \omega/\omega_0$ is the revolution harmonic number, $\omega_0 = 2\pi f_0$ is the revolution frequency.

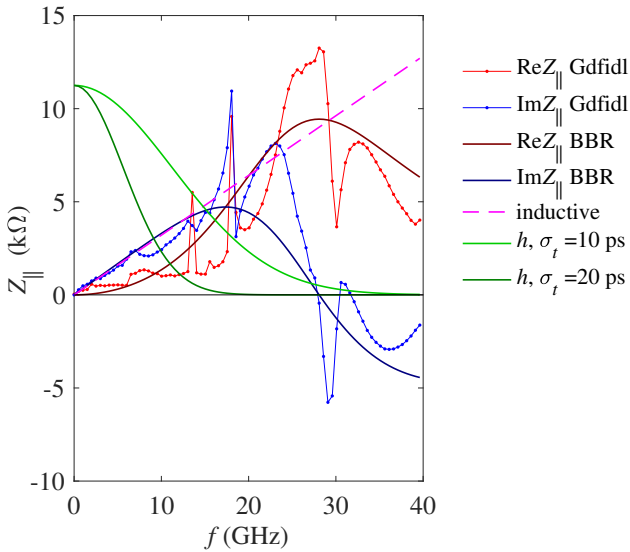


Figure 1: Longitudinal impedance of NSLS-II.

The measurable effects, such as intensity-dependent bunch lengthening and synchronous phase shift, are determined by the integral parameters: the normalized effective impedance

$$\left(\frac{Z_{\parallel}}{n} \right)_{\text{eff}} = \frac{\int_{-\infty}^{\infty} Z_{\parallel}(\omega) \frac{\omega_0}{\omega} h(\omega) d\omega}{\int_{-\infty}^{\infty} h(\omega) d\omega}, \quad (5)$$

and the energy loss factor

$$k_{\parallel} = \int_{-\infty}^{\infty} V_{\parallel}(t) \lambda(t) dt = \frac{1}{2\pi} \int_{-\infty}^{\infty} Z_{\parallel}(\omega) h(\omega) d\omega, \quad (6)$$

where $h(\omega) = \tilde{\lambda}(\omega) \tilde{\lambda}^*(\omega)$ is the bunch power spectrum.

For the bunch length of 10 ps, $(Z_{\parallel}/n)_{\text{eff}} = 0.117 \Omega$ and $k_{\parallel} = 50$ V/pC compared to the GdfidL data $(Z_{\parallel}/n)_{\text{eff}} = 0.119 \Omega$ and $k_{\parallel} = 45$ V/pC. For the bunch length of 20 ps, $(Z_{\parallel}/n)_{\text{eff}} = 0.127 \Omega$ and $k_{\parallel} = 6$ V/pC compared to the GdfidL data $(Z_{\parallel}/n)_{\text{eff}} = 0.131 \Omega$ and $k_{\parallel} = 9$ V/pC.

BEAM-BASED MEASUREMENTS

The longitudinal effective impedance can be estimated by fitting the measured bunch profile $\lambda(t)$ with the Haissinski equation [3]

$$\lambda(t) = K \lambda_0(t) \exp \left(\frac{I_b}{\omega_s \sigma_{\delta} \frac{E}{e}} \int_{-\infty}^t dt'' \int_{-\infty}^{\infty} dt' W_{\parallel}(t'' - t') \lambda(t') \right), \quad (7)$$

or by fitting the measured bunch length σ_t with the cubic equation [2]

$$\left(\frac{\sigma_t}{\sigma_{t0}} \right)^3 - \frac{\sigma_t}{\sigma_{t0}} = \frac{I_b}{4\sqrt{\pi} \alpha \omega_0 \sigma_{t0} \sigma_{\delta}^2 E/e} \text{Im} \left(\frac{Z_{\parallel}}{n} \right)_{\text{eff}}, \quad (8)$$

where I_b is the beam current, ω_s is the synchrotron frequency, E is the beam energy, α is the momentum compaction factor, σ_{δ} is the relative energy spread, λ_0 is the bunch profile at zero intensity. The intensity-dependent bunch lengthening can be obtained from direct measurement of the bunch profile using a streak-camera, or from indirect measurement of the bunch length using a button-type pickup electrode.

Coherent energy loss caused by the beam-impedance interaction results in an intensity-dependent shift of the synchronous phase ϕ_s :

$$\Delta\phi_s = \frac{I_b k_{\parallel}}{f_0 V_{\text{RF}} \cos \phi_{s0}}, \quad (9)$$

where V_{RF} is the RF voltage, ϕ_{s0} is the synchronous phase at zero current. So the loss factor k_{\parallel} can be estimated by fitting the measured phase shift $\Delta\phi_s$ with formula (9). Note the loss factor k_{\parallel} depends on the bunch length increasing with the beam current, so the phase shift (9) is a non-linear function of the beam current. The synchronous phase shift can be measured directly using several diagnostic instruments including synchrotron light diagnostics (streak-camera, dissector tube), RF system diagnostics or button-type pickups. To reduce the systematic error resulted from the drift or jitter of the diagnostic instruments, the reference-bunch technique is useful.

A series of precise measurements of the intensity-dependent bunch lengthening and synchronous phase shift was carried out at NSLS-II [6–8]. An example of the intensity-dependent bunch length measured with the operational NSLS-II lattice is presented in Figure 2. The experimental data are shown in comparison with the calculations using formulae (7, 8) applied to the simplified impedance models. The result of self-consistent simulations using the SPACE code [9] with the impedance computed by GdfidL, is also shown Figure 2. Figure 3 shows the measured synchronous phase shift (b) also compared to the formulae (7, 9) with simplified impedance models, as well as to the results of the SPACE simulations. The relevant machine and beam parameters are: $E = 3$ GeV, $\alpha = 0.000363$, $f_0 = 378.5$ kHz, $U_0 = 645$ keV, $f_{\text{rf}} = 499.68$ MHz, $V_{\text{rf}} = 3$ MV, $\phi_{s0} = 168^\circ$, $\nu_{s0} = 0.0086$, $\sigma_{\delta} = 9 \cdot 10^{-4}$, $\sigma_{t0} = 15.5$ ps.

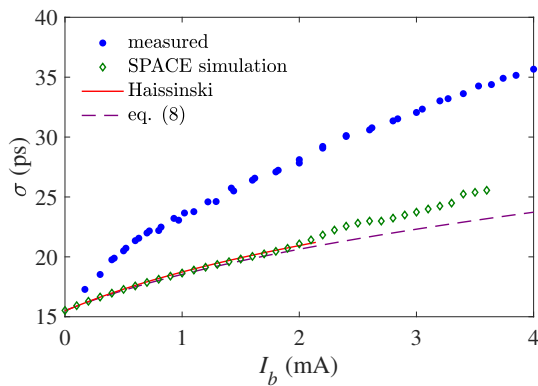


Figure 2: Intensity-dependent bunch length.

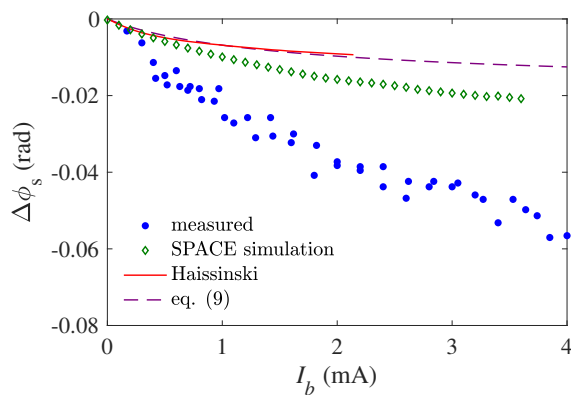


Figure 3: Intensity-dependent shift of synchronous phase.

As one can see, the results of self-consistent simulations are in agreement with the formulae applied to the simplified impedance models, however the measured data do not agree with the computations. So we can conclude the broadband longitudinal impedance of NSLS-II is underestimated.

CONCLUSION

As for other storage rings, the beam-based measurements of the broadband longitudinal impedance at NSLS-II show significant discrepancy with the pre-computed impedance budget. The experimental data were collected using several diagnostic instruments and measurement techniques, so the measurement accuracy looks sufficient. The reason for the discrepancy is still unclear, possible reasons are listed below.

- Components not included in the impedance budget. However, the most recent impedance budget of NSLS-II includes almost all components of the vacuum chamber except very few of them: 5 ceramic chambers, 3 scrapers, a septum chamber, and a DCCT.
- The effect of the computational mesh size should be small enough in the NSLS-II case because the mesh size used for simulations (30 – 50 μm) is much smaller (about 1/10) than the r.m.s. length of the model bunch. Furthermore, this effect is more significant for the high-frequency impedance rather than for the low-frequency one.

- Insufficient bandwidth of the computed impedance, if the length of a model bunch is not short enough. This error is minimized by using a model bunch of 0.3 mm length, which is at least 10 times shorter than the actual NSLS-II bunch.
- Interference of wake fields excited by a beam in neighboring components of a vacuum chamber. Experimental cross-check is proposed: measuring local impedance of one of high-impedance sections to compare with the impedance computed for the whole section vs a sum of element-by-element computations.
- For beam diagnostic devices, such as striplines and button pickups, the beam-induced power propagating out of the vacuum chamber via feedthroughs is not taken into account when the wake potential is calculated. However, this power can be quite significant as it was shown by recent measurements at NSLS-II [10]. So this effect could be one of possible reasons of the underestimated loss factor.

REFERENCES

- [1] V. Smaluk, “Impedance computations and beam-based measurements: A problem of discrepancy”, in *Nucl. Instrum. Methods Phys. Res.*, vol 888, pp. 22-30, Apr. 2018. doi:10.1016/j.nima.2018.01.047
- [2] R. Nagaoka, “Collective beam instabilities and methods of their suppression”, presented at High-Brightness Synchrotron Light Source Workshop, BNL, Upton, NY, USA, Apr. 2017.
- [3] J. Haissinski, “Exact longitudinal equilibrium distribution of stored electrons in the presence of self-fields”, in *Nuovo Cimento*, vol. B 18, 1973, pp. 72-82.
- [4] W. Bruns, “The GdfidL electromagnetic field simulator”, <http://www.gdfidl.de/>
- [5] A. Blednykh, “Impedance modelling in low emittance rings”, presented at International Workshop on Impedances and Beam Instabilities in Particle Accelerators, Benevento, Italy, Sept. 2017.
- [6] W. X. Cheng, B. Bacha, A. Blednykh, Y. Li, and O. Singh, “Longitudinal Bunch Profile Measurement at NSLS2 Storage Ring”, in *Proc. IBIC’15*, Melbourne, Australia, Sep. 2015, pp. 251–255. doi:10.18429/JACoW-IBIC2015-MOPB083
- [7] G. Bassi, A. Blednykh, J. Rose, V. V. Smaluk, and J. Tagger, “Synchronous Phase Shift from Beam Loading Analysis”, in *Proc. IPAC’17*, Copenhagen, Denmark, May 2017, pp. 3227–3229. doi:10.18429/JACoW-IPAC2017-WEPIK118
- [8] W. X. Cheng, B. Bacha, K. Ha, and O. Singh, “Precise Synchronous Phase Measurements”, in *Proc. IPAC’17*, Copenhagen, Denmark, May 2017, pp. 487–490. doi:10.18429/JACoW-IPAC2017-MOPAB152
- [9] G. Bassi, A. Blednykh and V. Smaluk, “Self-consistent simulations and analysis of the coupled-bunch instability for arbitrary multibunch configurations”, in *Phys. Rev. Accel. Beams*, vol. 19 (2016), p. 024401, Feb. 2016. doi/10.1103/PhysRevAccelBeams.19.024401
- [10] A. Blednykh *et al.*, to be submitted for publication.